ON THE GEOMETRIC POTENTIAL OF THE NMC DIGITAL CAMERA

J. Roig, M. Wis, I. Colomina

Institute of Geomatics, Parc Mediterrani de la Tecnologia, Av. del Canal Olímpic s/n, E-08860 Castelldefels, Spain - (joan.roig, mariano.wis, ismael.colomina)@ideg.es

KEY WORDS: camera calibration, digital photogrammetry, multihead modular camera, calibration performance analysis.

ABSTRACT:

In this paper we summarize the results of the investigation on the geometric precision potential of the New Metric Camera (NMC). The reported results cover geometric calibration, direct orientation and indirect orientation via block adjustment (without and with GPS, INS/GPS aerial control).

The NMC sensor is a new modular camera concept where a number of the so-called camera heads, up to three, can be combined. Each camera head is a high resolution 10000 x 1600 pixels (colour or infrared) sensor. This high resolution camera concept has been developed by Inpho GmbH and the reported analyses were conducted within the frame of the EU funded project GeoPIE (Geoinformation via Parallel Image Engineering).

The paper summarizes the outcome of an extensive modelling and simulation exercise carried out within GeoPIE. The results indicate that the NMC inherits many of the advantages of both frame cameras and line cameras. The NMC can be configured as monohead or multihead. When configured as a 2-head or 3-head camera its geometrical performance is comparable to that of large area frame cameras.

1. INTRODUCTION

1.1 The project

This paper summarizes a part of the research conducted by the Institute of Geomatics (IG) within the EU funded Geoinformation via Parallel Image Engineering (GeoPIE) project. A major component of the GeoPIE project was the development of a new digital camera prototype that materialized the modular, multihead concept of the New Metric Camera (NMC). One of the tasks was to develop the photogrammetric model for a set of camera heads as a whole and the corresponding ground (position) and aerial (position, velocity and attitude) control models. Subsequently, another task was to apply the models to the analysis of the NMC calibration, orientation and point determination precision accuracy.

1.2 Structure of the paper

Firstly, the main features and the particular geometry of the NMC are explained. The following section describes the imaging, geometric and control mathematical models. Then, the methodology of the analysis is explained focusing on the most influencing performance factors (dimensions of the problem). After that, the main results of the calibration, orientation and point determination of the NMC are shown and finally, the last section summarizes the conclusions of the reported work.

2. THE NMC CONCEPT

The NMC is a new metric digital camera that combines both the advantages of a frame camera and a line scanner. It is a modular system consisting of one or more camera heads (CH) located on the same platform or mount and looking at different directions. All CH are identical digital cameras.

2.1 General characteristics

The main NMC characteristics are summarized in table 1.

Parameter	Value
Focal length	48.9 mm
Field of view	48º
Pixel size	4.4 micron
Non-nadiral heads tilt	± 22.5º
Image size (per head)	10k x 1.6k pixel

Table 1 NMC characteristics

The inclination angle of forward (fw) and backward (bw) looking heads guarantees a close to 45º intersection angle at any point on the object surface.

2.2 Geometry concept

2.2.1 Internal geometry: as explained above, the NMC consists of 1, 2 or 3 CH placed on a rigid platform. When only 1 CH is in use the sensor works as a traditional frame camera. The combination with another CH allows for two different system configurations. In a symmetric assembly one head looks forward while the other one looks backward. The non-symmetric possibility, however, is to place one head into the nadir looking position and the other looking forward (or backward). The configuration that provides a stronger geometry (shown in figure 1) includes 3 CH, two tilted ones (backward-looking and forward-looking) and a nadir-looking one. The

mount is also prepared to hold an IMU as figure 1 depicts.

To deal with this internal geometry and to represent spatial data require the definition of reference systems and their practical realization, known as reference frames according to modern geodesy. For the definition of the mathematical models explained below the interest is focused on the following reference frames:

Frame m: instrumental cartesian reference frame with parametrization sequence Iflu (instrumental forward-left-up) which origin is the geometric centre of the mount.

Frame h_i: instrumental cartesian reference frame with parametrization sequence Iflu centred on the i^{th}-head.

Frame b: instrumental cartesian reference frame with parametrization sequence Ifrd (instrumental forward-right-down) centred on the IMU.

Frame l: Earth local cartesian reference frame with parametrization sequence Lenu (local east-north-up). The origin is a convenient fixed point on the Earth's surface.

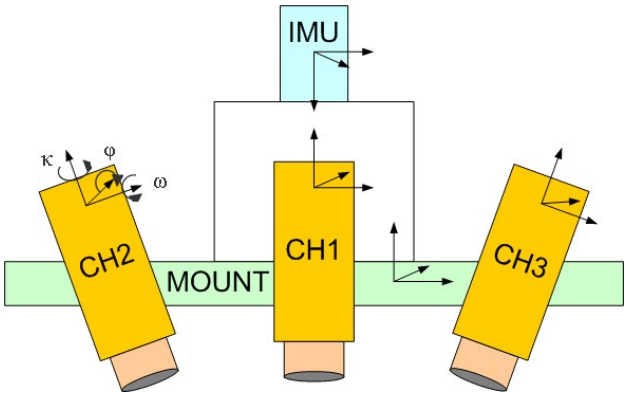

Figure 1. Internal geometry of the NMC

2.2.2 Acquisition geometry: the internal configuration of the system allows a particular acquisition geometry that takes advantage of the inclination of the backward and forward-looking heads. The goal is to take the images ensuring that the same ground area viewed by the first head (forward or nadir-looking) is, a few number of exposures later, viewed by another one. Figure 2 shows this geometry where the two mentioned exposures are called *bridge exposures*.

Notice that we talk about *exposures* rather than images. In fact, an exposure is a set of 1, 2 or 3 actual images that correspond to a configuration of 1, 2 or 3 NMC heads respectively. Thus, in a 3 CH configuration 1 exposure means that 3 actual images were taken.

Analogously to a stone bridge, the space between two consecutive exposures (a column in a bridge) is called *arc*. Therefore, the *number of arcs* corresponds to the number of exposures between two bridge ones (note that there is one exposure less than the number of actual arcs).

3. THE NMC IMAGING, GEOMETRIC AND CONTROL MODELS

The calibration and orientation performance analysis of the NMC by means of numerical simulations required the definition of some mathematical models describing the main features of the system.

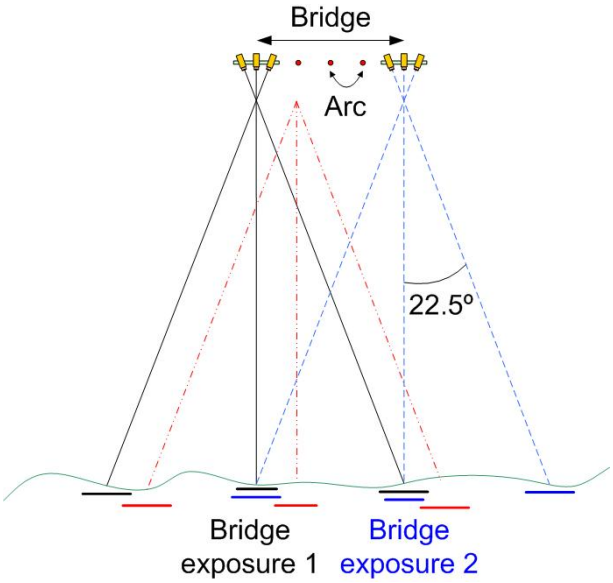

Figure 2. Flight geometry for a 3CH configuration

3.1 The photogrammetric model of the NMC

The classical photogrammetric model has been tailored to the particular internal geometry of the NMC. Its functional model is based on equation (1), which relates the image coordinates (p, q) in the image reference frame h_i to the ground points coordinates $(x, y, z)^T$ in the local terrestrial reference frame *l* subtracting the projection centre coordinates $(X, Y, Z)^T$,

$$\begin{bmatrix} p \\ q \\ -f \end{bmatrix}^{h_i} = \frac{1}{\lambda} R_{h_i}^{m\,-1} \cdot R_m^{l\,-1} \begin{bmatrix} x-X \\ y-Y \\ z-Z \end{bmatrix}^{l} - R_{h_i}^{m\,-1} \cdot t(h_i)^m \quad (1)$$

and where f is the focal length, λ is a scale factor, R^m_{hi} is the rotation matrix from the i^{th}-head reference frame to the mount reference frame, R^l_m is the rotation matrix from the *m* reference frame to the *l* reference frame (ω, φ, κ parametrization) and $t(h_i)^m$ is the eccentricity vector from the h_i reference frame to the mount's reference frame origin.

3.2 GNSS control model

This model deals with the time-dependent observations for the position of the mount given by a GNSS receiver. It is extended by shift and drift (SD) parameters to describe linear systematic errors in positioning as equation (2) shows:

$$x^l = X^l + R_m^l \cdot a^m + s^l + d^l \cdot (t - t_0) \quad (2)$$

where x^l is the vector with the coordinates x, y and z of the GNSS receiver antenna in the *l* reference frame, X^l is the projection centre vector in the *l* frame, a^m is the mount-to-GNSS antenna lever-arm in the *m* reference frame, s^l is the vector with the coordinates of the shift in position, d^l is the vector with the coordinates of the drift in position, t is the acquisition time and t_0 is the reference time for the drift (usually chosen as the central point in time of the GNSS strip).

3.3 INS / GNSS control model

When INS data is available (combined with GNSS data), a new model is necessary to relate this observations to the exterior orientation of the mount. Equations (3) and (4) define this model:

$$x^l = X^l + R_b^l \cdot \left[R(q) \cdot R(\alpha,\beta,\gamma)\right]_m^b \cdot b^m + s^l + d^l \cdot \left(t - t_0\right) \quad (3)$$

$$R_m^l = R_b^l \cdot \left[R(q) \cdot R(\alpha,\beta,\gamma)\right]_m^b \quad (4)$$

where R^l_b is the rotation matrix from the *b* reference frame to the *l* reference frame, $[R(q)\cdot R(\alpha,\beta,\gamma)]^b_m$ is the rotation matrix from the *m* frame to the *b* frame – R(q) is a 3x3 constant matrix (through 4 components of a quaternion) and R(α,β,γ) is the actual rotation matrix from *m* to *b* where (α,β,γ) are the orientation angles of the IMU with respect to the mount) – and b^m is the mount-to-IMU lever-arm.

Equation (3) relates the trajectory of the IMU with the trajectory of the mount (similarly as equation (2) does with the trajectory of the GNSS antenna and the mount) whereas equation (4) relates the orientation of the IMU with the orientation of the mount.

4. METHODOLOGY OF THE ANALYSIS

The main goal of the reported work was the analysis of the calibration, orientation and point determination performance of the NMC. Under calibration, or determination of the interior orientation of the CH, we mean the determination of the relative orientations and displacements of each CH with respect to the mount. This calibration is related to the determination of the camera constants (focal length and principal point coordinates) as well. The orientation refers to the determination of the position and attitude of the NMC and point determination refers to the position of the ground points.

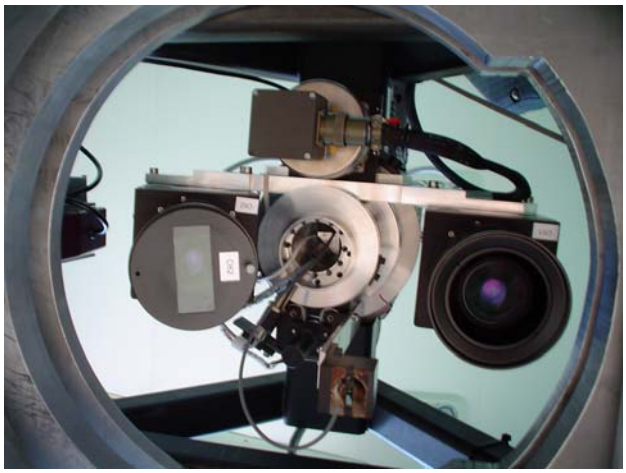

Figure 3. Bottom view of the NMC in a 2CH configuration (left and right in the image) and 1 IMU (centre up)

This analysis was performed by means of numerical simulations. Hence, more than 40.000 simulations were carried out where all the input data were simulated values as well.

To perform all those simulations implied a previous work. Thus, the first step was the definition and development of the mathematical models explained in the above section. Once they were implemented, a rigorous simulation plan was prepared. This was done by identifying the so-called dimensions of the problem, i.e. the most influencing performance factors, summarized in table 2.

Finally, in parallel with the simulations, the last step was to analyze the results and to compare them. These results are described in the following sections.

Acronym	Dimension	Range / Values
NMCC	NMC configuration	1 CH, 2 CH (nadir & forward-looking), 2 CH (backward & forward-looking), 3 CH
BSS	Block size and shape	Size: from 5 to 42 exposures Shape: only forward strips / forward and cross strips, just bridge images / all consecutive images
GCD	Ground control distribution	No GCP (ground control points), 1, 2, 4 and 8 GCP, first and last point of each strip, full GCP distribution (all of the points are GCP)
GCPP	Ground control point precision	5, 10 & 20 cm
IOD	Image observations distribution	3 x 1 (image observations distributed along one central column), 3 x 3 (similar to a Von Gruber distribution)
IOP	Image observations precision	1 / 2 pixel, 1 / 10 pixel
ACAP	Aerial control attitude precision	Navigation grade A & B IMUs (high cost), tactical grade IMU (medium cost), automotive grade types I & II IMUs (low cost), no IMU
ACPP	Aerial control position precision	5, 10 & 20 cm, no GNSS receiver
ACPA	Aerial control position accuracy	SD parameters fixed, SD parameters not fixed, shift free and drift fixed
CC	Camera calibration (only for orientation analysis purposes)	Navigation grade A IMU calibration, navigation grade B IMU calibration, tactical grade IMU calibration

Table 2. Dimensions of the NMC calibration and orientation

5. RESULTS

In this paper, we will only provide a snapshot of the more than 40000 simulations performed. For the sake of clarity, the results in the calibration and orientation are sorted according to the impact of the variation of each dimension. For this purpose, we have selected the most representative configuration for each of the cases and then we present the results in tables according to that configuration.

We also remark that not all the possible combinations of the values shown in table 2 were simulated as there are some of them that make no sense (for example an analysis of the calibration performance without GNSS receiver and without IMU).

5.1 Calibration results

The analysis of the calibration performance is focused on the 3 orientation angles of each head with respect to the mount. In all the tables presented in this section (except table 3) the results for both tilted heads are shown in the same column because, as they have the same inclination with respect to the vertical axis of the *m* reference frame in absolute value (22.5º), their calibration precision is also the same. All the results in the following tables are shown in arc seconds.

For the optimal configurations, i.e. the ones that lead to best results, the standard deviation of these angles is about 2 arc seconds (1-sigma level). The precision in the results is always better for the nadiral CH than for the tilted ones and the determination of the κ angle is always less precise than the other two angles.

5.1.1 NMC configuration: as expected, the results obtained for the 4 analysed cases are very similar. Therefore, even if only one CH is available the calibration is possible with a similar precision compared to a 3CH configuration as represented in table 3:

NMCC	Nadir			Forward			Backward		
	σ_ϖ	σ_φ	σ_κ	σ_ϖ	σ_φ	σ_κ	σ_ϖ	σ_φ	σ_κ
1	3.3	3.3	6.7						
2 nd & fw	3.3	3.3	6.2	4.1	3.5	6.7			
2 fw & bw				4.1	3.7	6.8	4.1	3.7	6.8
3	3.3	3.2	6.0	4.0	3.4	6.5	4.0	3.4	6.5

Table 3. Calibration precision depending on NMCC

5.1.2 Block size and shape: the precision of calibration has a strong dependence on block size. It is clear that, the bigger the block is the more precise is the calibration. On the other hand, block shape only affects the results for the weakest geometries (low values for the other dimensions). Therefore, the calibration performance is nearly independent of the block shape.

A small number of simulations were performed with just bridge exposures. Flying over the same area, the results are poor compared to those of all consecutive exposures due to the less number of total images as we can see in table 4:

Block shape	Nadir			Fw & Bw		
	σ_ϖ	σ_φ	σ_κ	σ_ϖ	σ_φ	σ_κ
5 x 17	2.36	2.28	3.49	2.77	2.29	3.79
5 x 5 bridge exp.	4.12	3.88	6.28	4.85	3.96	6.77

Table 4. Calibration precision depending on block shape

5.1.3 Ground control distribution: the number and distribution of GCP has almost no effect on the calibration for all the optimal configurations. In fact, the precision in the determination of the ω and φ angles of each head remains nearly constant whatever the GDC is whereas its impact in the determination of the κ angle is a bit higher. Table 5 shows one of the optimal configurations where the no necessity of GCP is clear.

GCPD	Nadir			Fw & Bw		
	σ_ϖ	σ_φ	σ_κ	σ_ϖ	σ_φ	σ_κ
No GCP	1.68	1.55	2.67	2.01	1.57	2.90
1 GCP	1.68	1.55	2.67	2.01	1.57	2.90
2 GCP	1.68	1.55	2.67	2.01	1.57	2.90
4 GCP	1.67	1.55	2.61	2.00	1.57	2.84
8 GCP	1.67	1.55	2.58	1.98	1.56	2.80
Full GCP dist.	1.68	1.54	2.38	1.93	1.53	2.59

Table 5. Calibration precision depending on GCPD

5.1.4 Ground control points precision: for calibration purposes the only GCPP taken into account was 5 cm because of the low number of points and the small size of the blocks.

5.1.5 Image observations distribution: it is difficult to isolate the calibration precision depending only on the IOD because the results are also strongly dependant on the IOP and the ACPP. Nevertheless, in general terms the differences in precision for the two analyzed IOP are not greater than 1.5 arc seconds. Moreover, for the optimal configurations this difference is negligible.

5.1.6 Image observations precision: this dimension has an important impact on the calibration, especially in the determination of κ. Although this effect is less significant for the other two head-to-mount angles it is still important.

When there are no GCP, which is the case depicted in table 6, it is necessary to keep this value as high as possible; otherwise, the obtained precision is not enough to properly calibrate the NMC. Therefore, the calibration of the sensor should be performed over areas with good image texture.

IOP	Nadir			Fw & Bw		
	σ_ϖ	σ_φ	σ_κ	σ_ϖ	σ_φ	σ_κ
1 / 2 pixel	2.91	2.94	9.07	3.73	4.49	9.22
1 / 10 pixel	2.81	2.69	5.54	3.48	3.05	5.71

Table 6. Calibration precision depending on IOP

An improvement in the IOD also helps to reduce, but not minimize, the differences in the precision of the results between 1/2 pixel and 1/10 pixel IOP.

5.1.7 Aerial control attitude precision: the IMU quality is one of the dimensions that have the biggest influence in the final results. Thus, sensor calibration is not possible with automotive grade IMUs due to the fact that the precisions for the interior orientation of the CH are even lower than 100 arc seconds.

Furthermore, the precision with a navigation grade A IMU is about two times better than for a tactical grade IMU. Nevertheless, this last type of IMU suffices for optimal

configurations. Otherwise, a navigation grade IMU should be required.

ACAP	Nadir			Fw & Bw		
	σ_ϖ	σ_φ	σ_κ	σ_ϖ	σ_φ	σ_κ
Nav. A	1.70	1.62	2.88	2.05	1.76	3.06
Nav. B	2.21	2.15	3.48	2.62	2.28	3.71
Tact.	3.12	3.07	5.67	3.89	3.17	6.11
Aut. I	35.2	35.1	104.9	55.9	35.1	113.4
Aut. II	116.7	115.4	228.0	151.0	115.4	246.7

Table 7. Calibration precision depending on ACAP

It is apparent that no simulations were carried out without an IMU.

5.1.8 Aerial control position precision: although this dimension severely affects the results when analyzing the other ones, the calibration is possible even with a low precision GNSS receiver for good geometries.

5.1.9 Aerial control position accuracy: setting the shift-and-drift parameters for GNSS and INS data results in a significant improvement in the calibration precision with respect to estimating them. Particularly, the low precision in the determination of ω when SD parameters are adjusted does not allow the calibration of the camera as shown in table 8:

ACPA	Nadir			Fw & Bw		
	σ_ϖ	σ_φ	σ_κ	σ_ϖ	σ_φ	σ_κ
No SD	2.52	2.38	3.94	3.04	2.66	4.19
SD	18.92	2.54	4.75	19.28	2.82	8.86

Table 8. Calibration precision depending on ACPA

When there is no possibility to fix SD parameters, then cross strips combined with a 3 x 3 IOD are necessary as they reduce the lack of precision in the determination of ω. Table 9 shows the results for a similar number of exposures and free SD parameters where 3 x 21 means that 21 exposures have been taken at each one of the 3 flown strips and 3 x 9fw – 3 x 9cr refers to a flight with 3 forward and 3 cross strips and 9 exposures per strip:

Block shape	Nadir			Fw & Bw		
	σ_ϖ	σ_φ	σ_κ	σ_ϖ	σ_φ	σ_κ
3x9fw-3x9cr	3.19	2.93	4.86	3.77	2.88	5.30
3x21	19.75	2.91	5.83	20.09	3.10	9.72

Table 9. Calibration precision for free SD parameters and 3x3 IOD comparing flights with and without cross strips

5.2 Orientation and point determination results

The analysis in this section consists of the comparison of the standard deviations (1-sigma level) of the position and attitude of the mount and also the coordinates of the ground points. The results are presented in tables where the minimum, maximum, mean and RMS values of the standard deviations are shown in meters (position and points) and arc seconds (attitude).

The optimal results in the determination of the position are about 0.05 m (mean), 5 arc seconds for the attitude and 0.035 m for the points.

5.2.1 NMC configuration: the precision of orientation and point determination does not depend on the NMCC for 2 and 3 CH. Not surprisingly, the results are poorer with only 1 CH, especially in the estimation of the vertical components. The precision in the attitude severely decreases for the κ angle as well.

5.2.2 Block size and shape: the main effort is focused on the comparison of the results between 20% and 60% cross overlap over the same area. Although the differences in precision for the position and points' determination are small, they can be higher than 1.5 arc seconds for the attitude. Furthermore, when cross overlap is 20% the orientation of the sensor is not possible with automotive grade IMUs because of the bad precision in the determination of ω (unless having a high number of GCP).

5.2.3 Ground control distribution: this dimension is strongly related to the ACPA. Thus, when SD parameters are fixed (GNSS positions regarded as free of systematic errors) the resultant standard deviations are very similar whatever the GCD is and the orientation is even possible, though not recommended without GCP.

	Exterior Orientation						Ground Points		
Full GCP dist	σ_X	σ_Y	σ_Z	σ_ϖ	σ_φ	σ_κ	σ_x	σ_y	σ_z
Min.	0.034	0.048	0.015	6.518	4.537	2.279	0.008	0.008	0.016
Max.	0.044	0.060	0.023	8.017	5.822	3.444	0.024	0.022	0.040
Mean	0.037	0.052	0.017	6.930	4.896	2.635	0.014	0.013	0.025
RMS	0.037	0.052	0.017	6.939	4.907	2.653	0.014	0.014	0.026
8 GCP									
Min.	0.048	0.067	0.047	8.276	5.352	2.767	0.023	0.024	0.045
Max.	0.064	0.089	0.059	11.494	7.586	5.790	0.071	0.065	0.103
Mean	0.054	0.076	0.051	9.579	6.209	3.916	0.041	0.041	0.064
RMS	0.054	0.076	0.051	9.616	6.240	3.984	0.043	0.042	0.066

Table 10. Orientation and point determination depending on GCD

	Exterior Orientation						Ground Points		
5 cm	σ_X	σ_Y	σ_Z	σ_ϖ	σ_φ	σ_κ	σ_x	σ_y	σ_z
Min.	0.041	0.052	0.038	5.838	4.782	3.139	0.022	0.023	0.042
Max.	0.052	0.062	0.045	7.698	6.542	5.761	0.062	0.058	0.094
Mean	0.045	0.056	0.040	6.505	5.401	4.048	0.037	0.037	0.054
RMS	0.046	0.056	0.040	6.523	5.423	4.099	0.038	0.038	0.056
10 cm									
Min.	0.051	0.061	0.051	5.909	4.810	3.251	0.038	0.038	0.053
Max.	0.062	0.070	0.056	7.771	6.581	5.800	0.070	0.067	0.099
Mean	0.056	0.064	0.052	6.575	5.443	4.152	0.050	0.050	0.064
RMS	0.056	0.064	0.052	6.593	5.466	4.202	0.051	0.050	0.065
20 cm									
Min.	0.080	0.086	0.080	5.953	4.837	3.338	0.072	0.072	0.082
Max.	0.088	0.094	0.084	7.826	6.609	5.831	0.094	0.091	0.117
Mean	0.083	0.089	0.081	6.627	5.475	4.226	0.080	0.080	0.089
RMS	0.083	0.089	0.081	6.647	5.500	4.276	0.080	0.080	0.090

Table 11. Orientation and point determination depending on GCPP

On the other hand, when SD parameters are estimated the orientation is not possible without GCP and there is a high impact in the precision of the attitude having a small number of GCP as shown in table 10.

5.2.4 Ground control points precision: despite of the precision in the estimation of the attitude slightly decreases when the GCPP is worsened, the precision in the position and points determination is reduced by a factor of 2 (difference between 5 cm and 20 cm GCPP). Nevertheless, table 11 shows that even if the GCPP is 20 cm the precision is good enough for the orientation of the sensor.

5.2.5 Image observations distribution: while the precision in the position is almost not affected by this dimension, the precision in the attitude is reduced for a 3 x 1 IOD, particularly in the determination of the ω angle as depicted in table 12. This reduction is minimized when the IMU is replaced with a high cost one.

5.2.6 Image observations precision: when the less optimal configurations are simulated, the orientation is not possible with a 1/2 pixel IOP. However, this dimension is strongly related to the IOD. With a good IOP, then a good IOD is not required and vice versa.

In general terms, IOP has a stronger effect in the determination of the attitude and the coordinates of the points than in the estimation of the position.

5.2.7 Aerial control position precision: the orientation of the NMC requires an airborne GNSS receiver unless the number of GCP is very high. Nevertheless, a good performance in the orientation of the NMC is possible whatever the ACPP is except for low cost IMUs and bad IOP.

5.2.8 Aerial control attitude precision: note, as it was to be expected, that for configurations with good geometry, precisions in orientation and point determination are good enough even without an IMU. Thus, the standard deviations of the position of the mount and the points are independent of the IMU quality for the best possible configurations as table 13 shows. There is only a significant difference in the estimation of the attitude, especially for ω.

When the other dimensions get worse values then at least a tactical grade IMU is required. The position is always estimated with enough precision, whereas the standard deviation of the attitude angles is rapidly made worse for low cost IMUs.

5.2.9 Aerial control position accuracy: in some optimal configurations the precision in the results is independent of the ACPA. However, when only low cost IMUs are available it is necessary to fix drift parameters at least due to an important decrease in the precision in the attitude.

5.2.10 Camera calibration: the way the camera heads are calibrated does not have a strong effect in the results for the orientation. Thus, the precision in the trajectory, attitude and ground point determination slightly depends on the calibration (for optimal configurations).

6. CONCLUSIONS

In general terms it seems that the NMC concept inherits many, if not most, of the good properties of line cameras and frame cameras. Once the camera is calibrated, it behaves similarly to a frame camera.

Calibration procedures are specific to the camera, and good head-to-head calibration, as it was to be expected, can be achieved by the use of tactical or navigation grade IMUs without the use of GCP.

7. ACKNOWLEDGEMENTS

The research reported in this paper has been done in the context of the EU funded GeoPIE project (ref: IST-1999-57456). We thank the many colleagues of Inpho, VTT, SILO, REAB, PIEneering, Hansa Luftbild and the IG that have contributed with their expertise to the project. In particular we thank Marta Blázquez for her assistance in the simulations and Edgar Aigner for his management of the project at the IG.

	Exterior Orientation						Ground Points		
3 x 1	σ_X	σ_Y	σ_Z	σ_ϖ	σ_φ	σ_κ	σ_x	σ_y	σ_z
Min.	0.061	0.112	0.070	13.661	6.747	4.749	0.040	0.041	0.067
Max.	0.076	0.136	0.079	17.882	9.611	9.412	0.083	0.092	0.147
Mean	0.067	0.122	0.073	15.430	7.698	6.460	0.057	0.061	0.091
RMS	0.067	0.123	0.073	15.481	7.735	6.576	0.058	0.062	0.094
3 x 3									
Min.	0.048	0.065	0.052	7.222	4.700	3.240	0.036	0.037	0.054
Max.	0.058	0.082	0.061	10.144	6.119	4.399	0.115	0.103	0.264
Mean	0.052	0.072	0.054	8.341	5.071	3.528	0.041	0.042	0.065
RMS	0.052	0.072	0.054	8.381	5.081	3.537	0.042	0.043	0.071

Table 12. Orientation and point determination depending on IOD

	Exterior Orientation						Ground Points		
Navigation A IMU	σ_X	σ_Y	σ_Z	σ_ϖ	σ_φ	σ_κ	σ_x	σ_y	σ_z
Min.	0.038	0.043	0.035	4.665	4.253	2.268	0.022	0.022	0.037
Max.	0.048	0.051	0.039	5.708	5.301	5.029	0.056	0.052	0.090
Mean	0.042	0.046	0.036	5.015	4.608	3.224	0.034	0.034	0.049
RMS	0.042	0.046	0.036	5.022	4.617	3.297	0.035	0.034	0.051
Navigation B IMU									
Min.	0.040	0.046	0.036	5.232	4.542	2.400	0.022	0.022	0.040
Max.	0.050	0.056	0.042	6.746	6.021	5.250	0.059	0.055	0.092
Mean	0.044	0.050	0.038	5.753	5.055	3.411	0.036	0.035	0.052
RMS	0.044	0.050	0.038	5.766	5.072	3.484	0.037	0.036	0.053
Tactical IMU									
Min.	0.041	0.051	0.038	5.813	4.697	2.678	0.022	0.023	0.042
Max.	0.052	0.061	0.045	7.685	6.486	5.546	0.062	0.058	0.094
Mean	0.045	0.055	0.040	6.483	5.328	3.710	0.037	0.037	0.054
RMS	0.045	0.055	0.040	6.501	5.351	3.777	0.038	0.038	0.056
Automotive type I IMU									
Min.	0.042	0.071	0.044	8.823	4.855	2.945	0.022	0.024	0.044
Max.	0.054	0.085	0.052	11.376	6.987	5.787	0.065	0.060	0.097
Mean	0.047	0.077	0.047	9.873	5.620	3.982	0.039	0.038	0.062
RMS	0.047	0.077	0.047	9.900	5.652	4.043	0.040	0.040	0.063
Automotive type II IMU									
Min.	0.042	0.072	0.044	8.945	4.856	2.946	0.022	0.024	0.044
Max.	0.054	0.086	0.052	11.507	6.991	5.788	0.065	0.060	0.098
Mean	0.047	0.077	0.047	10.000	5.623	3.983	0.039	0.038	0.062
RMS	0.047	0.078	0.047	10.027	5.655	4.043	0.040	0.040	0.063
No IMU									
Min.	0.043	0.073	0.045	9.128	5.102	2.949	0.022	0.024	0.044
Max.	0.056	0.088	0.054	11.790	7.419	5.840	0.067	0.062	0.099
Mean	0.049	0.079	0.048	10.223	5.933	4.019	0.040	0.040	0.063
RMS	0.049	0.079	0.048	10.251	5.970	4.081	0.041	0.041	0.064

Table 13. Orientation and point determination depending on ACAP